Preclinical Study of the Systemic Toxicity and Pharmacokinetics of 5-Iodo-2-deoxypyrimidinone-2′-deoxyribose as a Radiosensitizing Prodrug in Two, Non-Rodent Animal Species: Implications for Phase I Study Design[1]

Timothy J. Kinsella,[2] Jane E. Schupp, Thomas W. Davis, Suzanne E. Berry, Hwa-Shin Hwang, Kathy Warren, Frank Balis, John Barnett, and Howard Sands

Department of Radiation Oncology, Case Western Reserve University and University Hospitals of Cleveland/Ireland Cancer Center, Cleveland, Ohio 44106-6068 [T. J. K., J. E. S., T. W. D., S. E. B., H-S. H.]; Clinical Pharmacology Section, Pediatric Oncology Branch, National Cancer Institute, Bethesda, Maryland 20892 [K. W., F. B.]; Argus Research Laboratories, Inc., Horsham, Pennsylvania 19044 [J. B.]; and SuperGen Pharmaceuticals, San Ramon, California 94583 [H. S.]

ABSTRACT

We have demonstrated previously an improved therapeutic index for oral 5-iodo-2-deoxypyrimidinone-2′-deoxyribose (IPdR) compared with oral and continuous infusion of 5-iodo-2′-deoxyuridine (IUdR) as a radiosensitizing agent using three different human tumor xenografts in athymic mice. IPdR is a prodrug that is efficiently converted to IUdR by a hepatic aldehyde oxidase, resulting in high IPdR and IUdR plasma levels in mice for ≥1 h after p.o. IPdR. Athymic mice tolerated oral IPdR at up to 1500 mg/kg/day given four times per day for 6–14 days without significant systemic toxicities. In anticipation of an investigational new drug application for the first clinical Phase I and pharmacology study of oral IPdR in humans, we studied the drug pharmacokinetics and host toxicities in two non-rodent, animal species.

For the IPdR systemic toxicity and toxicology study, twenty-four male or female ferrets were randomly assigned to four IPdR dosage groups receiving 0, 15, 150, and 1500 mg/kg/day by oral gavage × 14 days prior to sacrifice on study day 15. All ferrets survived the 14-day treatment. Ferrets receiving 1500 mg/kg/day showed observable systemic toxicities with diarrhea, emesis, weight loss, and decreased motor activity beginning at days 5–8 of the 14-day schedule. Overall, both male and female ferrets receiving IPdR at 1500 mg/kg/day experienced significant weight loss (9 and 19%, respectively) compared with controls after the 14-day treatment. No weight loss or other systemic toxicities were observed in other IPdR dosage groups. Grossly, no anatomical lesions were noted at complete necropsy, although liver weights were increased in both male and female ferrets in the two higher IPdR dosage groups. Histologically, IPdR-treated animals showed dose-dependent microscopic changes in liver consisting of minimal to moderate cytoplasmic vacuolation of hepatocytes, which either occurred in the periportal area (high dosage group) or diffusely throughout the liver (lower dosage groups). Female ferrets in the highest IPdR dose group also showed decreased kidney and uterus weights at autopsy without any associated histological changes. No histological changes were found in central nervous system tissues. No significant abnormalities in blood cell counts, liver function tests, kidney function tests, or urinalysis were noted. Hepatic aldehyde oxidase activity was decreased to approximately 50 and 30% of control ferrets in the two higher IPdR dosage groups, respectively, after the 14-day treatment period. The % IUdR-DNA incorporation in ferret bone marrow at the completion of IPdR treatment was ≤0.05% in the two lower dosage groups and ≅2% in the 1500 mg/kg/day dosage group. The % IUdR-DNA in normal liver was ≤0.05% in all IPdR dosage groups.

In a pharmacokinetic study in four Rhesus monkeys, we determined the plasma concentrations of IPdR after a single i.v. bolus of 50 mg/kg over 20 min. Using a two-compartment model to fit the plasma pharmacokinetic data, we found that IPdR was cleared in these non-human primates in a biexponential manner with an initial rapid distributive phase (mean $T_{1/2}\alpha$ = 6.5 min), followed by an elimination phase with a mean $T_{1/2}\beta$ of 63 min. The mean maximum plasma concentration of IPdR was 124 ± 43 μM with a mean total body clearance of 1.75 ± 0.95 l/h/kg. IPdR was below detection (<0.5 μM) in the cerebrospinal fluid.

We conclude that there are dose-limiting systemic toxicities to a 14-day schedule of p.o. IPdR at 1500 mg/kg/day in ferrets that were not found previously in athymic mice. However, no significant hematological, biochemical, or histopathological changes were found. Hepatic aldehyde oxidase activity was reduced in a dose-dependent in ferret liver, suggesting partial enzyme saturation by this IPdR schedule. The plasma pharmacokinetic profile in Rhesus monkeys showing biexponential clearance is similar to our published data in athymic mice. These data are being applied to the

Received 4/17/00; revised 6/13/00; accepted 6/13/00.

The costs of publication of this article were defrayed in part by the payment of page charges. This article must therefore be hereby marked *advertisement* in accordance with 18 U.S.C. Section 1734 solely to indicate this fact.

[1] Supported in part by NIH Grant RO-1 CA50595 (to T. J. K., J. E. S., T. W. D., S. E. B., and H-S. H.) and NIH Small Business Innovation Research Grant R44-CA76835 (to T. J. K. and H. S.).

[2] To whom requests for reprints should be addressed, at Department of Radiation Oncology, University Hospitals of Cleveland/Ireland Cancer Center, LTR 6068, Room B-181, 11100 Euclid Avenue, Cleveland, OH 44106-6068. Phone: (216) 844-2530; Fax: (216) 844-4799.

design of an initial clinical Phase I study of p.o. IPdR as a radiosensitizer.

INTRODUCTION

IUdR[3] is a dThd analogue that has been recognized for several decades as an effective *in vitro* and *in vivo* radiosensitizer using various mouse and human tumor cell lines (1, 2). IUdR cellular metabolism and radiosensitizing effects are dependent on the dThd salvage pathway with initial phosphorylation to IdUMP by the rate-limiting enzyme, thymidine kinase, followed by sequential phosphorylation to IdUTP, which competes effectively with dTTP for DNA incorporation by DNA polymerase (1). Indeed, DNA incorporation is a prerequisite for tumor radiosensitization, and the extent of radiosensitization (up to 3-fold using *in vitro* clonogenic survival and induction of double-strand DNA breaks) correlates directly with the percentage of dThd replacement by IUdR in DNA (3–5). The molecular mechanisms of radiosensitization are related to an increased susceptibility of IUdR-substituted dThd bases in DNA to the generation of highly reactive uracil-free radicals caused by IR, which may also damage unsubstituted complementary-strand DNA (6, 7). Repair of IR damage in tumor cells may also be reduced by prior exposure to these analogues (8, 9). More recently, we have reported that human tumor and murine embryonic stem cells deficient in DNA MMR, related to lack of expression of either MLH1 or MSH2 proteins, show significantly greater IUdR-DNA incorporation and IUdR-related radiosensitization than genetically matched MMR-proficient cells (10, 11). This selective radiosensitization in MMR-deficient ($MLH1^-$ or $MSH2^-$) human tumors by IUdR may be exploited clinically because these MMR-deficient tumors are resistant to many commonly used chemotherapeutic agents (12), including 5-fluorouracil and cisplatin, which are also commonly used as clinical radiosensitizers (1, 2).

Because IUdR is rapidly metabolized by hepatic and extrahepatic routes when given by bolus infusion (plasma $T_{1/2} < 5$ min) in both rodents and humans (1), a prolonged continuous or intermittent i.v. schedule is necessary to maximize the proportion of tumor cells that incorporate IUdR during S-phase. Using a human colon cancer xenograft model, we found that 95–99% of the tumor cells incorporated IUdR into DNA after a continuous exposure for approximately five times the potential tumor doubling time (T_{pot}; Ref. 13), which is measured to be in the range of 2–8 days for many human tumors (1). Recent Phase I and II clinical trials using prolonged continuous or repeated intermittent i.v. infusions of IUdR or the related analogue 5-bromo-2′-deoxuridine in clinically radioresistant human tumors including high-grade brain tumors, locally advanced squamous cell cancers of the cervix or head and neck, locally advanced sarcomas, and colorectal liver metastases suggest a therapeutic gain in clinical radiosensitization using these dThd analogues (14–21). However, systemic toxicity to rapidly proliferating normal tissues (principally bone marrow and intestine) can limit the duration and dose rate of the drug infusion and consequently may limit the extent of human tumor radiosensitization by the halogenated dThd analogues (14–21).

The use of p.o. administered IPdR as a prodrug for IUdR-mediated tumor radiosensitization is an experimental approach under development by our group over the last 5 years (22–24). The original strategy for development of pyrimidinone nucleosides like IPdR by Efange *et al.* (25) was based on the hypothesis that nucleosides without an amino group or oxygen at position 4 would be used as substrates by viral thymidine kinase but not by mammalian cellular nucleoside kinases. While screening several 5-substituted 2-pyrimidinone-2′-deoxyribonucleoside analogues for anti-herpes simplex virus activity in HeLa cell cultures, IPdR was found to be most effective (26). Importantly, IPdR was also found to have significant activity in herpes simplex-infected mice, even with oral (p.o.) administration, and was associated with no significant host toxicities (26). Although these initial studies suggested that p.o. IPdR did not require metabolism to IUdR for antiviral activity, follow-up studies by these same investigators found an aldehyde oxidase present in both mouse and rat liver that efficiently converts IPdR to IUdR (27). Other normal rodent tissues including intestine, bone marrow, lung, brain, and kidney showed ≥1 log less activity of this IPdR-aldehyde oxidase.

In three recent publications, we have documented an improved therapeutic gain for *in vivo* human tumor xenograft radiosensitization in athymic mice using daily p.o. dosing of IPdR × 6–14 days compared with either daily p.o. or continuous infusion IUdR for similar time periods using MTD schedules of IUdR (22–24). Using two different human colon cancer cell lines (HT-29 and HCT 116) and one human glioblastoma cell line (U251) as s.c. xenografts in athymic mice, we found ≥2-fold increases in % IUdR-DNA tumor cell incorporation and ≥2-fold decreases in % IUdR-DNA incorporation in proliferating dose-limiting normal tissues (bone marrow and intestine) after p.o. IPdR compared with either p.o. or continuous infusion IUdR. Pharmacokinetic analyses in mice of p.o. IPdR showed efficient metabolism of IPdR to IUdR by hepatic IPdR aldehyde oxidase with peak plasma levels of the prodrug (IPdR) and active drug (IUdR) noted within 15 min of p.o. IPdR administration and measurable IPdR and IUdR plasma levels for up to 90–120 min (22, 23). Using cytosolic extracts from normal human liver specimens, we also found rapid *in vitro* conversion of IPdR to IUdR, suggesting that normal human liver has significant IPdR-aldehyde oxidase activity. This human hepatic enzyme activity was protein dependent and inhibited by low concentrations of menadione and isovanillin (selective inhibitors for aldehyde oxidase) but not with allopurinol (a selective inhibitor of xanthine oxidase; Ref. 23). In contrast to human liver, normal human small intestine was found to have significantly lower (>1 log) IPdR-aldehyde oxidase activity, similar to our mouse data (22, 23). IPdR-aldehyde oxidase activity was not detectable in cytosolic extracts from two specimens of human colorectal cancer and from the two human colorectal tumor xenografts (23). Finally, using a tumor regrowth assay to assess IR response, we found a 1.3–1.5-fold enhancement (time to

[3] The abbreviations used are: IUdR, 5-iodo-2′-deoxyuridine; IPdR, 5-iodo-2-pyrimidine-2′-deoxyribose; CSF, cerebrospinal fluid; dThd, thymidine; IR, ionizing radiation; MMR, mismatch repair; MTD, maximum tolerated dose; AUC, area under the curve; CMC, carboxymethyl cellulose; HPLC, high-performance liquid chromatography; qd, four times per day.

regrow to 300% initial tumor volume) with IPdR (qd × 6–14 days) plus fractionated IR (2 Gy/day × 4 days) in both human colorectal and glioblastoma xenografts compared with fractionated IR alone (22, 24). Less (≤1.1) enhancement of the IR response was found using continuous infusion IUdR × 6–14 days plus fractionated IR in these human tumor xenografts (23, 24).

On the basis of these promising *in vivo* data using human tumor xenografts in athymic mice (22–24), we extend our preclinical evaluation of oral IPdR to include toxicology and drug metabolism studies in two non-rodent animal species and summarize the data in this report. Collectively, the rodent and non-rodent data will allow us to design the initial clinical Phase I and pharmacology study of p.o. IPdR as a radiosensitizer.

MATERIALS AND METHODS

Drugs. IPdR ($CaH_{11}N_2O_4I$) was synthesized and provided by SuperGen Pharmaceuticals, Inc. (San Ramon, CA). CMC was obtained from Sigma Chemical Co. (St. Louis, MO) as a white powder. Aqueous 0.5% CMC was prepared as the vehicle for oral IPdR administration in ferrets using reverse osmosis, membrane-processed deionized water. The aqueous 5% CMC vehicle was stored refrigerated, and the IPdR was dissolved and prepared each day of administration for the ferret toxicity study. For the plasma and cerebrospinal fluid pharmacokinetic studies in Rhesus monkeys, IPdR was dissolved in 17% 2-hydroxypropyl-β-cyclodextrin (Sigma) and prepared fresh on the day of study for i.v. administration.

Animals. The Marshall Farms ferret (North Rose, NY) was selected as a non-rodent species for IPdR systemic toxicity and toxicology testing. Twelve male and 12 female ferrets, ages 4–6 months, and weighing 1.1–1.5 kg (male) or 0.7–0.9 kg (female) were randomly assigned to four IPdR dosage groups including three ferrets per sex per group. The ferrets were individually housed in stainless steel cages and provided ~75 g of Marshall Premium Ferret Diet (Marshall Farms, North Rose, NY) each day and water *ad libitum* with chlorine added as a bacteriostatic. The IPdR toxicity study in these ferrets was conducted in compliance with Good Laboratory Practice regulations of the Food and Drug Administration (28) and the Organization for Economic Cooperation and Development (29).

Four adult male Rhesus monkeys (*Macaca mulatta*), weighing 11.4–12.4 kg, were used for the plasma and CSF pharmacokinetics studies of a single i.v. dosing of IPdR. The monkeys were fed Purina Monkey Chow and water *ad libitum* and were group housed in accordance with the Guide for the Care and Use of Laboratory Animals (30). Blood samples were drawn through a catheter placed in either the femoral or the saphenous vein contralateral to the site of i.v. IPdR administration. CSF samples were drawn from a s.c. Ommaya reservoir attached to an in-dwelling Pudenz catheter with its tip located in the fourth ventricle, as described previously (31). This study was approved by the NIH Animal Care and Use Committee.

Drug Dosage. The four IPdR dosage groups in the ferret toxicity study included 0, 15, 150, and 1500 mg/kg/day (groups I–IV, respectively) with the same dosage volume of 10 ml/kg by oral gavage given once daily for 14 consecutive days. Dosages were adjusted daily for body weight changes and given at approximately the same time each day. The dosage range and schedule of dosing were based on prior preclinical studies of IPdR in athymic mice (22–24). The oral route was selected for the systemic toxicity and toxicology study because it is the proposed route for clinical use.

For the plasma and CSF pharmacokinetic studies of IPdR in Rhesus monkeys, each animal received 50 mg/kg IPdR prepared in 17% 2-hydroxypropyl-β-cyclodextrin (Sigma) to a total volume of 50 ml and infused i.v. over 20 min. Plasma samples were collected prior to infusion of IPdR; at the end of infusion; and 5, 10, 15, 30, 60, and 90 min and 2, 3, 4, 6, 8, 10, and 24 h after the end of the infusion. CSF samples were collected prior to infusion; at the end of infusion; and 0.5, 1, 1.5, 2, 3, 4, 6, 8, 10, and 24 h after the end of infusion. Plasma and CSF were frozen at −70°C until analysis.

Assessment of Systemic Toxicities during the 14-Day IPdR Treatment Schedule in Ferrets. Body weights were recorded three times prior to IPdR treatment, daily during the 2-week IPdR dosage period, and on the day of sacrifice (study day 15). Feed consumption values were recorded daily × 1 week prior to IPdR treatment, daily during the 2-week IPdR dosage period, and on study day 15 prior to sacrifice. All ferrets were observed for viability at least twice daily during treatment, typically prior to the daily gavage and 1 h after drug administration.

Blood samples were collected prior to study and prior to sacrifice (day 15) after the 14-day IPdR treatment. Approximately 2 ml of blood was collected via the jugular vein from each study ferret on both days of sample collection. Prior to sample collection, the ferrets were anesthetized by an i.m. injection of xylazine (3.2 mg/kg; the Butler Co., Columbus, OH) and ketamine (25 mg/kg; Fort Dodge Animal Health, Fort Dodge, IA). Approximately 1 ml of blood was collected into EDTA-coated tubes for analysis of the following hematological parameters: RBC, Hgb, Hct, mean corpuscular hemoglobin, MCHC, WBC, differential leukocyte count, platelet count, mean platelet volume, and cell morphology. Approximately 1 ml of blood was collected into serum separator tubes and centrifuged. The resulting sera samples were analyzed for the following: Na^+, K^+, Cl^-, Ca^{2+} PO_4^-, blood urea nitrogen, creatinine, glucose, cholesterol, triglycerides, total protein, albumin, total bilirubin, alkaline phosphatase, alanine aminotransferase, aspartate aminotransferase, and gamma glutamyl transpeptidase.

Prior to the start of the study and prior to necropsy (study day 15), urinalysis was conducted on all ferrets. Ferrets were hydrated by oral gavage with 100 ml of deionized water prior to the start of the urine collection period and deprived of feed and water during the collection period. Urine was collected in aluminum foil trays for ~6 h or until an adequate urine sample was obtained for evaluation but for no longer than 12 h. The following parameters were measured or calculated from the urine sample: color, pH, specific gravity, glucose, ketones, bilirubin, urobilinogen, nitrite, leukocytes, RBC, and microscopic examination of the sediment.

Gross Necropsy Study in Ferrets. All ferrets were sacrificed on study day 15 using an i.v. injection of pentobarbital sodium (~1 ml/ferret), following induction of anesthesia with an i.m. injection of xylazine/ketamine, as described previously.

At necropsy, gross lesions were retained in neutral buffered 10% formalin and examined histologically.

Gross necropsy included an initial physical exam of external surfaces and all orifices as well as an internal examination of tissues and organs *in situ*. The following were examined: external and internal portions of all hollow organs; the external surfaces of the brain and spinal column, the nasal cavity and neck, with associated organs and tissues; the thoracic, abdominal, and pelvic cavities, with associated organs and tissues; and the musculoskeletal carcass. The lungs were perfused with neutral buffered 10% formalin. The following organs were weighed prior to fixation: kidneys, liver, adrenal glands, uterus, ovaries, testes, and brain, with the paired organs weighed as pairs. The following tissues or representative samples were collected from all male and/or female ferrets at necropsy and retained in neutral buffered 10% formalin: adrenal glands, testes, ovaries, aorta (thoracic and abdominal), oviducts, bone marrow (femur), pancreas, gallbladder, large intestine (cecum, colon, and rectum), small intestine (duodenum, jejunum, and ileum), liver, stomach, spleen, uterus, cervix/vagina, kidneys, urinary bladder, prostate, epididymides, lymph nodes (mesenteric and mediastinal), mammary glands (one right and one left abdominal), lungs, heart, trachea, larynx/pharynx, thyroid and parathyroid, thymus, esophagus, tongue, salivary gland (submaxillary), pituitary, brain, spinal cord (mid-thoracic), sciatic nerve, skeletal muscle (quadriceps and femurs), skin (abdominal), and femur (including articular surface).

Histological examinations were performed in selected tissues from control (group I) ferrets and from ferrets in the three IPdR dosage groups (groups II–IV). The following organs or representative samples were submitted for histological evaluation: gross lesions, lung, heart, liver, stomach, small intestine, large intestine, kidney, uterus, ovaries, testes, brain, and spinal cord. Additionally, representative samples of bone marrow (entire femur) and liver (≥2 g)were immediately frozen after sacrifice in all ferrets to determine the % IUdR-DNA incorporation (bone marrow and liver) and the IPdR-aldehyde oxidase activity (liver) after the 14-day treatment period.

Measurement of % IUdR-DNA Incorporation in Ferret Bone Marrow and Liver. Approximately 500 mg of frozen ferret liver were chipped from each frozen organ with a mortar and pestle on dry ice. The samples were thawed on ice in 400 μl of PBS. Liver tissue was minced briefly with scissors and then sonicated on ice for 10 s three times with 10-s rests between pulses. Approximately 500 mg of bone marrow were taken from frozen femurs and processed similarly to liver tissue. DNA was extracted and digested by the method of Belanger *et al.* (32). The digestion mixture was incubated overnight at 34°C. Four-hundred-μl samples were ultra-filtered using Millipore ultrafree-MC units (Millipore Corp., Bedford, MA).

HPLC analysis of IUdR replacement of dThd in DNA from ferret liver and bone marrow samples were performed with the use of a Waters 600 E solvent delivery system on a 3.9 × 300-mm μBondapak reverse-phase column (Waters Corp., Milford, MA). Peak elution was monitored using a Waters 490 E UV detector. The system was controlled, and data were analyzed using Millenium Chromatography Manager, Version 2.10. Using the method of Belanger *et al.* (32), the mobile phase consisted of 100 mM sodium acetate buffer (pH 5.45) plus 7% (v/v) acetonitrile. dThd and IUdR were detected at 290 nm. Peak identification and quantitation were performed against authentic nucleoside standards (Sigma). Enzymes for DNA digestion were also obtained from Sigma. The % IUdR-DNA incorporation was calculated as:

$$\%\ \text{IUdR DNA incorporation} = \frac{\text{IUdR}}{\text{dThd} + \text{IUdR}} \times 100$$

Measurement of Hepatic IPdR-Aldehyde Oxidase Activity in Ferrets. At necropsy, liver tissue was immediately harvested and frozen until analysis of IPdR-aldehyde oxidase activity from all four ferret IPdR-dosage groups. Liver cytosols were prepared from frozen ferret liver samples (≅1 g) by chipping frozen pieces of liver from the whole frozen organ with a mortar and pestle on dry ice. Samples were thawed on ice in 400 μl of homogenization buffer consisting of 50 mM Tris-HCl (pH 7.5), 1 mM ATP-$MgCl_2$, and 10% glycerol. Samples were minced briefly with scissors before sonicating on ice three times for 10-s pulses with 10-s rests between pulses. Samples were centrifuged at 10,000 × *g* for 20 min, the supernatant was removed to a fresh tube, and protein determinations were done by a standard biochemical assay.

Four hundred μg of each ferret liver extract sample were incubated in a total of 100 μl of reaction buffer consisting of 50 mM Tris-HCl (pH 8.0), 1 mM EDTA, and 0.2 mM $K_3Fe(CN)_6$, with 0.2 mM IPdR as substrate. Incubations were done at 37° for 1 h before stopping the reaction with 300 μl of methanol (100%). Samples were spun through ultra-free MC filters at 5000 × *g* for 40 min to remove protein and then evaporated to dryness. Samples were resuspended in 100 μl of HPLC running buffer, 100 mM ammonium acetate buffer (pH 6.8), with 6% acetonitrile. Eighty μl of each sample were analyzed by HPLC for IPdR-aldehyde oxidase activity. HPLC analyses of samples were conducted on a Waters system as described above. Samples were eluted with 100 mM ammonium acetate buffer (pH 6.8), which was filtered through a Whatman 0.2 μM nylon membrane filter before adding 6% acetonitrile. The absorbance of the eluate was monitored at 230 nM, with a flow rate of 2 ml/min. The exact molar concentrations of IPdR and IUdR were determined by making 10-fold dilutions of each and measuring the absorbance of the 100-fold dilution at A_{max} and dividing by the extinction coefficient for each separate compound. IPdR-aldehyde oxidase activity in ferret liver was expressed as the pmol of IUdR generated per hour per 300 μg of protein. Samples were quantified with standard curves for IUdR. All incubations were done in duplicate for each IPdR dosage group (0, 15, 150, and 1500 mg/kg/day × 14 days), based on gender.

Measurement of IPdR Plasma and CSF Levels in Rhesus Monkeys. IPdR concentrations in plasma and CSF were measured with a reverse-phase HPLC assay. Plasma samples and IPdR plasma standards underwent solid-phase extraction using Varian Bond Elut 3 ml C_{18} solid-phase extraction cartridges (Varian, Harbor City, CA). The extraction cartridges were wetted with 4 ml of methanol and washed with 4 ml of 50:50 (v/v) 50 mM ammonium acetate:50 mM acetic acid prior to application of the plasma standard or sample. After the plasma standard or sample was applied to the cartridge, it was washed

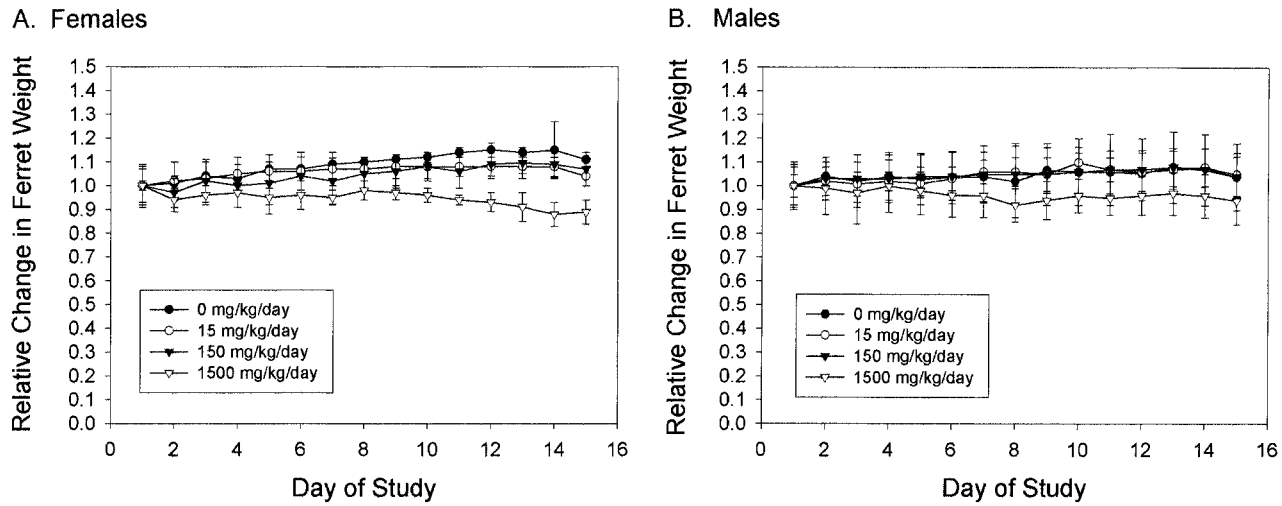

Fig. 1 Systemic toxicity as assessed by a change in ferret body weight measured daily during the 14-day p.o. IPdR treatment in both female (*A*) and male (*B*) ferrets is shown. The IPdR drug doses are illustrated on each panel. The change in body weights are normalized for each group of three, same-gender ferrets to the weights at day 1 prior to IPdR treatment; *bars*, SE.

with 2 ml of the 50:50 50 mM ammonium acetate:50 mM acetic acid buffer, and IPdR was eluted with 2 ml of methanol. The cartridge eluant was evaporated to dryness under a stream of nitrogen and reconstituted in 100 μl of the HPLC mobile phase. CSF samples were directly injected onto the column.

Extracted standards and samples were injected onto a μBondapak C18 column (Waters Corp.) with a μBondapak C18 guard column (Waters Corp.). The mobile phase consisted of 94:6 (v/v) 100 mM ammonium acetate:acetonitrile (pH 6.8), run isocratically at a flow rate of 1.5 ml/min. The HPLC system consisted of a Waters UltraWISP 715 sample processor, a Waters 510 pump, and a Waters 996 photodiode array detector. The column eluant was monitored at 232 and 288 nm. Analysis of the chromatograms was performed with Millenium software (Waters Corp.). For CSF, the limit of detection was 0.1 μM, and the coefficient of variation was ≤5%. For plasma, the lower limit of detection and the lower limit of quantification were 1.0 μM. The coefficient of variation was ≤12% for plasma concentrations ≥5 μM and 17.8% for the 1 μM concentration.

Pharmacokinetic Analysis of IPdR in Rhesus Monkeys. A two-compartment model, described by the following equations, was fit to the plasma concentration-time data using the mathematical modeling software program, MLAB (Civilized Software, Bethesda, MD):

$$\frac{dC_c}{dt} = \frac{k_0}{V_c} + \frac{k_{pc} \times X_p}{V_c} - k_{cel} \times C_c - k_{cp} \times C_c$$

and

$$\frac{dX_p}{dt} = k_{cp} \times C_c \times V_c - k_{pc} \times X_p$$

where C_c is the concentration of drug in the central compartment at time, t; X_p is the amount of drug in the peripheral compartment; k_o is the drug infusion rate; V_c is the volume of the central compartment; k_{cel} is the elimination rate constant; and k_{cp} and k_{pc} are the rate constants for exchange of drug between the central and peripheral compartments. Plasma AUC, total body clearance, and volume of distribution at steady state (*Vss*) were derived from the model parameters.

RESULTS

Clinical Observations in the Ferret Systemic Toxicity Study. All ferrets appeared normal and survived the 14-day treatment schedule of daily oral gavage in the control (vehicle alone; group I) and IPdR treatment groups (groups II–IV). Both male and female group IV (1500 mg/kg/day) ferrets showed decreased motor activity within 5 days of treatment, which was associated with ataxia and episodes of emesis in a majority of group IV animals by day 8 of treatment. Groups I–III ferrets showed normal motor activity and gait patterns without emesis throughout the 14-day treatment. Soft or liquid feces were noted in two group IV male ferrets on the last treatment day, and bradypnea was observed in one male and one female group IV ferret from days 10 to 14 of treatment. A change in bowel pattern or respiratory pattern was not observed in controls or the two lower IPdR dosage groups.

Body weight losses occurred in both male and female group IV ferrets throughout the 14-day treatment period (Fig. 1). No significant weight changes occurred in the two lower dosage IPdR groups (groups II and III) compared with the controls (group I). Body weight loss in group IV ferrets was more severe in females (19% at day 15; Fig. 1*A*) compared with males (9% at day 15; Fig. 1*B*). Absolute (g/day) and relative (g/kg/day) feed consumption values were reduced in male and female group IV ferrets compared with controls and with the two lower IPdR dosage groups. Feed consumption values were reduced in group IV ferrets for both the entire study period and for each study day comparison (complete data not shown). For example, the mean (± SD) absolute feed consumption values (g/day) for control (group I) male and female ferrets were 61.7 ± 6.9 and

Table 1 Selected organ weights in male and female ferrets after p.o. IPdR qd × 14 days

	IPdR dosage group			
	I	II	III	IV
IPdR dose (mg/kg/day)	0	15	150	1500
Liver weight (g) (mean ± SD)				
Male	40.9 ± 8.5	52.5 ± 9.3	61.5 ± 8.0	75.2 ± 6.6
Female	28.5 ± 3.9	31.0 ± 5.8	32.5 ± 1.9	37.3 ± 1.1
Uterus weight (g) (mean ± SD)				
Female	0.9 ± 0.2	0.6 ± 0.1	0.7 ± 0.2	0.4 ± 0.1
Kidney (paired) weight (g) (mean ± SD)				
Male	8.2 ± 0.9	8.2 ± 0.9	8.5 ± 0.3	9.2 ± 1.7
Female	6.2 ± 0.5	5.5 ± 0.7	5.2 ± 0.2	4.7 ± 0.3

56.1 ± 8.0 g/day for days 1–14 of treatment compared with values of 53.4 ± 11.6 and 37.2 ± 14.1 g/day for group IV male and female ferrets, respectively. The mean absolute feed consumption values for the two lower IPdR dosage groups (groups II and III) were not different from the control group. Thus, the observed body weight loss in group IV animals (Fig. 1) was correlated with a reduction in the absolute and relative feed consumption values compared with control (group I) and lower IPdR dosage groups (groups II and III).

Blood Test Analyses in the Ferret Systemic Toxicity Study. There were no abnormalities in the various hematological parameters, electrolytes, renal function (blood urea nitrogen and creatinine), glucose, lipids (cholesterol and triglycerides), proteins (albumin and total protein), and most liver function tests in all treatment groups (groups II–IV) compared with the controls (group I) after the 14-day treatment period. Lower mean posttreatment levels of certain liver enzyme tests (alanine aminotransferase, aspartate aminotransferase, and alkaline phosphatase) were noted in IPdR-treated ferrets compared with controls, but the SD overlapped for each test. Additionally, other liver function tests, including total bilirubin and gamma glutamyl transpeptidase, remained in a normal range after treatment in the IPdR-treated and control groups. No elevations in posttreatment liver function tests were found in the IPdR-treated ferrets compared with controls, indicating no acute compromise in liver function after the 14-day IPdR treatment.

Urinalysis in the Ferret Systemic Toxicity Study. A complete urinalysis, including color, pH, specific gravity, glucose, ketones, urobilinogen, bilirubin, nitrates, RBCs, WBCs, and microscopic examination of the sediment remained normal after IPdR (groups II–IV) and vehicle control (group I) treatments.

Necropsy Findings in the Ferret Systemic Toxicity Study. There were no gross lesions observed in any male or female ferret at necropsy in this study. The terminal body weights were reduced in all male and female group IV ferrets, in agreement with the observed body weight loss in the 1500 mg/kg/day dosage (group IV) throughout the 14-day treatment period (Fig. 1). In both male and female ferrets, the absolute liver weights were increased in a generally IPdR dosage-dependent manner in all treated groups. Additionally, the uterus weights were reduced in the 1500 mg/kg/day dosage group (group IV). Finally, the paired kidney weights were reduced in high-dose (group IV) female ferrets but not in male ferrets. The specific organ weights of liver and kidneys in both male and female ferrets as well as the uterus weights at necropsy in female ferrets for all four groups are presented in Table 1.

Histopathological Findings in the Ferret Systemic Toxicity Study. Possible treatment-related microscopic changes were observed only in the liver and stomach of male and female ferrets given 15, 150, or 1500 mg/kg/day of IPdR × 14 days (groups II–IV). The treatment-related histopathological change in the liver consisted of minimal to moderate cytoplasmic vacuolation of hepatocytes, which occurred either in the periportal areas or diffusely in all areas of hepatic lobules. The histological changes in liver in the high-dosage group (group IV) occurred predominantly in the periportal region, whereas diffuse cytoplasmic vacuolation was found more frequently in the two lower IPdR dosage groups (groups II and III). Using a four-grade histopathological scoring system (minimal, mild, moderate, and severe), only one of six group III ferrets had moderate diffuse cytoplasmic vacuolation. Two of six group IV ferrets also had moderate periportal vacuolation. No severe cytoplasmic vacuolation of hepatocytes in a diffuse or periportal pattern were observed in any of the IPdR-treated ferrets. No histopathological differences were noted in the livers between male and female ferrets in all three IPdR dosage groups.

Microscopic examination of the stomach also revealed possible treatment-related effects to the pyloric mucosa. Again, using a four-grade histopathological scoring system as above, the histopathological change was predominantly a mild to moderate superficial mucosal thinning with an associated mononuclear and polymorphonuclear inflammatory cell infiltration of the mucosa and submucosa. These changes occurred in all nine IPdR-treated male ferrets and seven of nine IPdR-treated female ferrets, but again, none was severe. No microscopic changes were found in the small and large intestine specimens submitted for histopathological review. Additionally, no microscopic changes occurred in the kidneys of group IV male and female ferrets or the uterus of group IV female ferrets, despite the observed lower organ weights at necropsy in these IPdR-treated animals (Table 1). Finally, no significant gross or microscopic changes were found in the central nervous system tissues at necropsy to possibly explain the clinically observed decreased motor activity noted in the high-dose IPdR group.

% IUdR-DNA Incorporation in Ferret Bone Marrow and Liver. Using the bone marrow as a surrogate of a proliferating normal tissue and liver as a surrogate of a nonproliferating normal tissue in ferrets, we measured the % IUdR-DNA incorporation in both of these normal tissues after the 14-day IPdR treatment. We were especially interested in the % IUdR-DNA incorporation in ferret liver because liver contains the highest levels of an aldehyde oxidase responsible for the conversion of IPdR to IUdR, as determined previously in the mouse and rat (22, 27). The % IUdR-DNA incorporation in ferret liver was very low and below detection (<0.05%) in IPdR-treated male and female ferrets. However, the % IUdR-DNA incorporation in ferret bone marrow increased in a dose-dependent fashion for the three IPdR dosage groups (Fig. 2). The % IUdR-DNA incorporation in bone marrow was not measurable

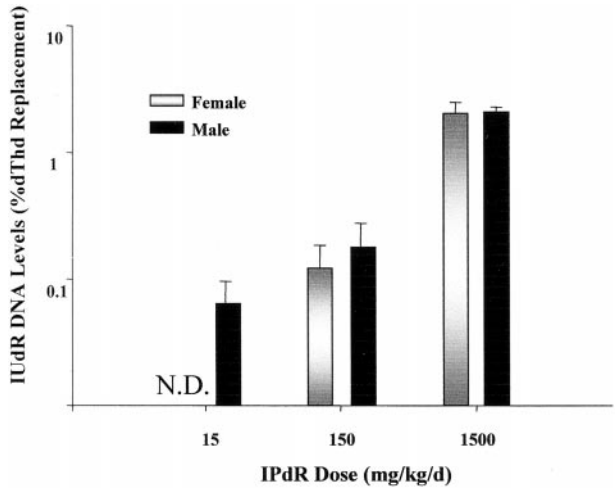

Fig. 2 % IUdR-DNA levels in male and female ferret bone marrow after the 14-day IPdR treatment based on the three dosage groups. The levels represent the bone marrow samples from three, same-gender ferrets in each IPdR dose group; *bars*, SE. *N.D.*, none detected.

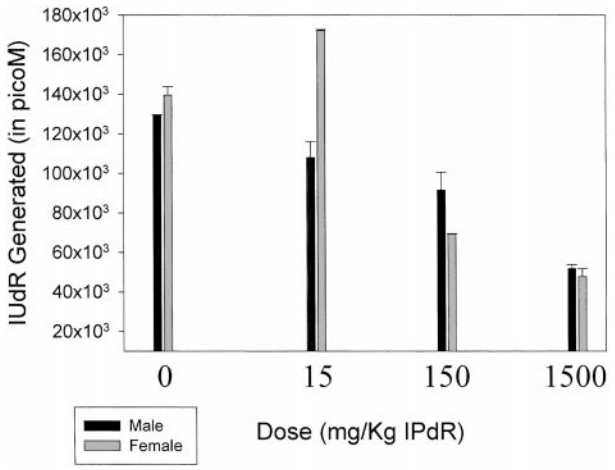

Fig. 3 Hepatic IPdR-aldehyde oxidase activity determined in liver cytosolic extracts from groups of three, same-gender ferrets in each IPdR dose group compared with the controls after the 14-day treatment; *bars*, SE. Each *column* represents enzyme activity from three same-gender ferrets. Enzyme activity is based on the *in vitro* conversion of IPdR to IUdR after a 1-h incubation of liver cytosolic extracts with IPdR.

in female ferrets and was only 0.06% in male ferrets after the lowest IPdR dose (15 mg/kg/day × 14 days) treatment. The % IUdR-DNA incorporation in bone marrow was also very low in group III ferrets, being only 0.1–0.2% after 150 mg/kg/day × 14 days. The level of 2.1 ± 0.3% found after IPdR treatment at 1500 mg/kg/day × 14 days is similar to the % IUdR-DNA incorporation found in normal bone marrow in athymic mice using the same dosage schedule (24). In both animal species, no changes in peripheral blood counts were found after the 14-day treatment. In contrast, myelosuppression (both low WBC and platelets) is one of the dose-limiting systemic toxicities in the clinical trials of the active drug, IUdR, when given as a prolonged continuous i.v. infusion for up to 14 days in humans (33). In these clinical trials of continuous infusion IUdR, the % IUdR-DNA incorporation in human peripheral granulocytes approached ≥10% at the MTD (34).

Hepatic IPdR-Aldehyde Oxidase Activity in Ferrets after the 14-day IPdR Treatment. We and others have shown previously that an aldehyde oxidase most concentrated in liver is responsible for the efficient conversion of IPdR to IUdR in mice, rats, and humans (22, 23, 27). The IPdR-aldehyde oxidase activity levels were ≥1 log higher in normal liver compared with other normal tissues (*e.g.*, intestine, brain, lung, and kidney) in these rodents and humans. However, aldehyde oxidase activity after IPdR treatment × 4–14 days has not been determined in our prior preclinical mouse studies (22–24). In this study, we determined the IPdR-aldehyde oxidase activity in cytosolic extracts from ferret liver taken at sacrifice on day 15 after the 14-day IPdR treatment. Enzyme activity was determined by measuring the *in vitro* conversion of IPdR to IUdR after a 1-h incubation of liver cytosolic extracts with IPdR (Fig. 3). Compared with control (group I) ferrets, we found an IPdR dose-related decrease in enzyme activity in both male and female ferrets, particularly with the two higher IPdR dosage schedules. There were significant reductions in enzyme activity to approximately 50 and 30% of controls after the 14-day treatment using 150 and 1500 mg/kg/day, respectively (Fig. 3).

IPdR Pharmacokinetics in Rhesus Monkeys. IPdR was cleared rapidly from plasma of the four monkeys with similar plasma IPdR concentration-time profiles after a single dose of 50 mg/kg as a 20-min i.v. infusion (Fig. 4). The peak plasma concentration was highest in animal 88003, who experienced lethargy after the infusion without other toxicities. No observable toxicity was found in the other three non-human primates.

The plasma concentration-time curves (Fig. 4) were biexponential with an initial rapid distributive phase (mean $T_{1/2}\alpha$, 6.5 min), followed by an elimination phase (mean $T_{1/2}\beta$, 63.0 min). A two-compartment model adequately described the disposition of IPdR in plasma in all four monkeys. The pharmacokinetic model parameters are listed in Table 2, and the standard pharmacokinetic parameters derived from the model parameters from each monkey are listed in Table 3 including the maximum plasma concentration (C_{max}), volume of distribution at steady state (*Vss*), plasma AUC, total body clearance, and elimination phase half-life ($T½\beta$). The mean values (± SD) are also calculated in Table 3. The plasma levels of IUdR could not be determined because of a conflicting HPLC peak in the monkeys. The IPdR concentration in the CSF was below the limit of quantification of the assay (*i.e.*, <0.5 μM) in all four monkeys. In one monkey, IUdR was detectable in the CSF at 1 h after the i.v. infusion but at a low concentration (1.5 μM).

DISCUSSION

In this preclinical study, we determined the dose-limiting systemic toxicities to a 14-day schedule of daily p.o. IPdR using ferrets as a non-rodent species. In contrast to our prior studies in athymic mice where no significant systemic toxicities were found with daily p.o. IPdR doses of up to 1500 mg/kg/day ×

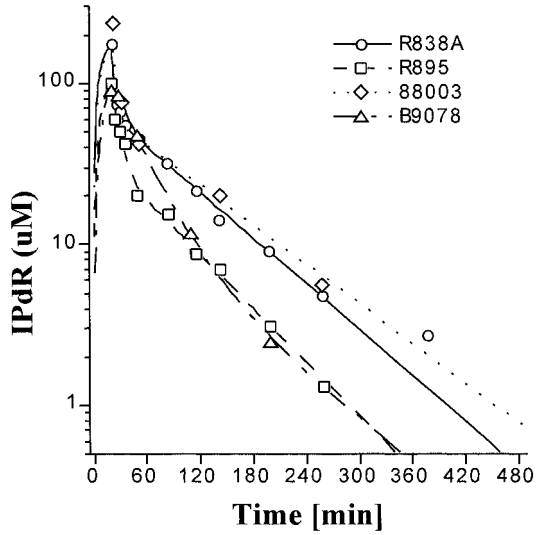

Fig. 4 Plasma IPdR concentration-time profiles in the four Rhesus monkeys after a 50-mg/kg dose of IPdR given as a 20-min i.v. infusion. The lines are the model fit to the data for each monkey (listed by number on figure) using a two-compartment model with first-order elimination from the central compartment.

Table 2 Fitted model parameters for a two-compartment model for IPdR plasma pharmacokinetics in four Rhesus monkeys that received IPdR (50 mg/kg i.v. over 20 min)

Monkey no.	V_c[a] (l/kg)	k_{cel} (min^{-1})	k_{cp} (min^{-1})	k_{pc} (min^{-1})
R838A	0.232	0.0740	0.155	0.0377
R895	0.641	0.0548	0.0585	0.0309
B9078	1.12	0.0438	0.00350	0.0127
88003	0.274	0.0563	0.103	0.0301
Mean[b]	0.565	0.0572	0.0800	0.0279
SD[b]	0.410	0.0125	0.0644	0.0107

[a] V_c, volume of the center compartment; k_{cel}, elimination rate constant; k_{cp}, rate constant for exchange between the central and peripheral compartment; k_{pc}, rate constant for exchange between the peripheral and central compartment.
[b] Mean value; standard deviation.

Table 3 IPdR pharmacokinetic parameters derived from the fitted model parameters (Table 2) in four Rhesus monkeys that received IPdR (50 mg/kg i.v. over 20 min)

Monkey no.	C_{max} (μM)	V_{ss} (l/kg)	AUC_{plasma} (μM·min)	Clearance (l/h/kg)	$T_{1/2}\beta$ (min)
R838A	174	1.18	8665	1.03	63.5
R895	98.5	1.86	4319	2.11	53.7
B9078	98.8	1.42	3045	2.93	60.5
88003	236	1.21	9653	0.924	73.6
Mean[a]	124	1.42	6420	1.75	62.8
SD[a]	43	0.31	3230	0.95	8.3

[a] Mean value; standard deviation.

6–14 days (22–24), we found significant weight loss (≥10% body weight; Fig. 1) and gastrointestinal side effects (emesis, diarrhea, and decreased feed consumption) in both male and female ferrets receiving 1500 mg/kg/day × 14 days. Although no toxic deaths were seen, we assigned the MTD for p.o. IPdR at ≤1500 mg/kg/day × 14 days in ferrets based on the measured weight loss and observed gastrointestinal toxicities. Mild to moderate microscopic histopathological changes were found in hepatocytes and in the superficial gastric mucosa in an IPdR dose-dependent manner. Additionally, although no gross anatomical lesions or other microscopic changes were noted at complete necropsy after the 14-day treatment period, there were increased liver weights in the two higher IPdR dosage groups (Table 1), but no biochemical liver function abnormalities were measured in serum. Direct quantification of the % IUdR-DNA incorporation in normal hepatocytes was below detection (<0.05%). Thus, the observed microscopic changes in liver and stomach may result from direct toxicity of the prodrug, IPdR. We will carefully monitor gastrointestinal and hepatic toxicities in the proposed clinical Phase I study.

Similar to our studies of p.o. IPdR in athymic mice, the % IUdR-DNA cellular incorporation in normal bone marrow remained quite low (≤2%; Fig. 2), and no myelosuppression was found in complete blood count analyses after IPdR treatment in all ferret groups. The low % IUdR-DNA bone marrow incorporation and no evidence of myelosuppression in both mice and ferret species using IPdR presumably results, in part, from ≥1 log lower levels of aldehyde oxidase in normal bone marrow compared with normal liver, as measured previously (27). As such, we do not anticipate that bone marrow toxicity will be the principal dose-limiting normal tissue in our proposed clinical trial of p.o. IPdR, although myelosuppression will be carefully monitored and peripheral circulating granulocytes will be collected for determination of % IUdR-DNA incorporation as a surrogate for a proliferating normal tissue (bone marrow), as used in our prior clinical studies of i.v. IUdR (33, 34). In the proposed Phase I study of p.o. IPdR, we anticipate a delay of 7–10 days from the start of p.o. IPdR to measure bone marrow effects (change in peripheral blood counts; detection of % IUdR-DNA incorporation in circulating granulocytes) and will monitor these effects for up to 4 weeks after the qd × 14-day schedule.

As part of this preclinical study of IPdR, we also analyzed IPdR metabolism in both non-rodent species. In the ferret study, we measured *in vitro* IPdR-aldehyde oxidase activity in cytosolic extracts from normal liver after the 14-day p.o. IPdR treatment. We found significant reduction in enzyme activity to 50 and 30% of normal controls in the two higher IPdR dosage groups but no significant gender differences (Fig. 3). These data suggest enzyme saturation with the repeated daily IPdR dose schedule used. In a recent published study in athymic mice, we found that a single p.o. dose of 1000 mg/kg IPdR decreased hepatic IPdR-aldehyde oxidase recovery to ~50% of control at day 1 after drug administration with full recovery to normal enzyme activity by day 2 (24). In the Rhesus monkey study, we measured the plasma pharmacokinetics of IPdR using a single i.v. administration of 50 mg/kg. Here, we found high (>100 μM) plasma concentrations at the end of the 20-min infusion with rapid biexponential clearance over 6–8 hours (Fig. 4). The plasma pharmacokinetic profile for IPdR is similar to our prior studies in athymic mice (22, 23). After a single p.o. bolus

administration of 250-1500 mg/kg IPdR in athymic mice, we found peak IPdR plasma concentrations of up to 250 μM within 20 min with efficient conversion of the prodrug, IPdR, to the active metabolite, IUdR, within 15–20 min. In athymic mice, peak plasma IUdR concentrations of 40–75 μM were measured at 20 min, and IUdR plasma concentrations persisted at >20 μM for up to 90 min (23). Unfortunately, in the Rhesus monkey study, plasma IUdR concentration could not be determined because of a conflicting HPLC peak. Surprisingly, no CSF penetration of the prodrug was found in the Rhesus monkey model.

On the basis of these pharmacokinetic data in Rhesus monkeys and our data published previously in athymic mice (22, 23), we conclude that oral or i.v. IPdR is rapidly cleared from plasma in a biexponential fashion (Fig. 4). However, it is evident that IPdR oxidase activity is saturable after high (>1000 mg/kg) single doses in mice (23, 24) and after repeated daily doses over 2 weeks in ferrets (Fig. 3). Collectively, these rodent and mammalian data of IPdR indicate the need for a careful, human pharmacokinetic study of p.o. IPdR as part of the initial Phase I clinical trial. We have already determined that normal human liver has significant IPdR-aldehyde oxidase activity (23). Human liver IPdR-aldehyde oxidase is cytosolic, protein dependent, and cofactor independent (23). It is inhibited by low concentrations of menadione and isovanillin but not allopurinol (23). Menadione and isovanillin are selective inhibitors for aldehyde oxidase, whereas allopurinol is a selective inhibitor for xanthine oxidase. Thus, our results indicate that a human hepatic aldehyde oxidase but not a hepatic xanthine oxidase is involved in the conversion of IPdR to IUdR. It is reported recently that kinetically distinct forms of aldehyde oxidase exist in male and female rodent liver that occur as a result of differences in redox state and not in cDNA sequencing (35, 36). However, a gender difference in enzyme activity as defined by *in vitro* conversion of IPdR to IUdR was not evident in ferrets (Fig. 2) or in our prior studies in athymic mice (24–24). A high degree of homology exists between mouse and human aldehyde oxidase (37). It is also recognized that differences in aldehyde oxidase activity are found between cytosolic preparations of human and monkey liver (38), which may limit the direct translation of our male Rhesus monkey data to the human trial.

On the basis of the systemic toxicity data using 1500 mg/kg/day × 14 days in ferrets, we propose a starting p.o. IPdR dose of 85 mg/m^2 qd × 14 days (≅1/10 MTD) in humans for the initial Phase I trial. We will compare the drug pharmacokinetics using both an i.v. formulation and p.o. formulation of IPdR to determine the absolute oral bioavailability. On the basis of the observed gastrointestinal toxicity seen in the ferret study and the higher % IUdR-DNA levels in normal intestine compared with normal bone marrow found in our previously published IPdR studies in athymic mice (22–24), we will carefully monitor patients for gastrointestinal toxicity using the National Cancer Institute common toxicity criteria. Again, we have already determined that human small intestine has significantly lower IPdR oxidase activity (≥10-fold reduction) compared with normal human liver (23). Similar to our Phase I studies using continuous i.v. infusions of IUdR as a radiosensitizing drug (33), daily p.o. IPdR will start at least 1 week prior to initiation of radiation therapy to affect radiosensitization.

REFERENCES

1. Kinsella, T. J. An approach to the radiosensitization of human tumors. Can. J. Sci. Am., *2:* 184–193, 1996.

2. McGinn, C. J., Shewach, D. S., and Lawrence, T. S. Radiosensitizing nucleosides. J. Natl. Cancer Inst., *88:* 1193–1203, 1996.

3. Kinsella, T. J., Dobson, P. P., Mitchell, J. B., and Fornace, A. J. Enhancement of x-ray induced DNA damage by pretreatment with halogenated pyrimidine analogs. Int. J. Radiat. Oncol. Biol. Phys., *13:* 733–739, 1987.

4. Lawrence, T. S., Davis, M. A., Maybaum, J., Stetson, P. L., and Ensminger, W. D. The dependence of halogenated pyrimidine incorporation and radiosensitization on the duration of drug exposure. Int. J. Radiat. Oncol. Biol. Phys., *18:* 1393–1398, 1990.

5. Miller, E. M., Fowler, J. F., and Kinsella, T. J. Linear-quadratic analysis of radiosensitization by halogenates pyrimidines. I. Radiosensitization of human colon cancer cells by iododeoxyuridine. Radiat. Res., *131:* 81–89, 1992.

6. Fornace, A. J., Dobson, P. P., and Kinsella, T. J. Enhancement of radiation damage in cellular DNA following unifilar substitution with iododeoxyuridine. Int. J. Radiat. Oncol. Biol. Phys., *18:* 873–878, 1990.

7. Lawrence, T. S., Davis, M. A., Maybaum, J., Stetson, P. L., and Ensminger, W. D. The effect of single *versus* double stranded substitution on halogenated pyrimidine-induced radiosensitization and DNA strand breakage in human tumor cells. Radiat. Res., *123:* 192–198, 1991.

8. Wang, Y., and Iliakis, G. Effects of 5′-iododeoxyuridine on the repair of radiation induced potentially lethal damage, interphase chromatin breaks, and DNA double strand breaks in Chinese hamster ovary cells. Int. J. Radiat. Oncol. Biol. Phys., *23:* 353–360, 1992.

9. Schultz, C., Gaffney, D., Lindstrom, M., and Kinsella, T. J. Iododeoxyuridine radiosensitization of human glioblastoma cells exposed to acute and chronic gamma irradiation: mechanistic implications and clinical relevance. Can. J. Sci. Am., *1:* 151–161, 1995.

10. Berry, S. E., Garces, C., Hwang, H-S., Kunugi, K., Myes, M., Davis, T. W., Boothman, D. A., and Kinsella, T. J. The mismatch repair protein, hMLH1, mediates 5-substituted halogenated thymidine analogue cytotoxicity, DNA incorporation, and radiosensitization in human colon cancer cells. Cancer Res., *59:* 1840–1845, 1999.

11. Berry, S. E., Davis, T. W., Schupp, J. E., deWind, N., and Kinsella, T. J. Selective radiosensitization of drug-resistant, MSH2 mismatch repair deficient cells by the halogenated thymidine (dThd) analogs: MSH2 mediates dThd analog DNA levels and the differential cytotoxicity and cell cycle effects of the dThd analogs and 6-TG. Cancer Res., in press, 2000.

12. Fink, D., Aebi, S., and Howell, S. The role of DNA mismatch repair in drug resistance. Clin. Cancer Res., *4:* 1–6, 1998.

13. Rodriquez, R., Ritter, M. A., Fowler, J. F., and Kinsella, T. J. Kinetics of cell labeling and thymidine replacement after continuous infusion of halogenated pyrimidines *in vivo*. Int. J. Radiat. Oncol. Biol. Phys., *29:* 105–113, 1994.

14. Urtasun, R., Kinsella, T., Farnam, N., DelRowe, J., Lester, S., and Fulton, D. Survival improvement in anaplastic astrocytoma combining external radiation with halogenated pyrimidines: final report of RTOG 86-12, Phase I-II study. Int. J. Radiat. Oncol. Biol. Phys., *36:* 1163–1167, 1996.

15. Prados, M., Scott, C., Rotman, M., Rubin, P., Murray, K., Sause, W., Asbell, S., Comis, R., Curran, W., Nelson, J., Davis, R., Levin, V., Lamborn, K., and Phillips, T. Influence of bromodeoxyuridine radiosensitization on malignant glioma patient survival: a retrospective comparison of survival data from the Northern California Oncology Group (NCOG) and Radiation Therapy Oncology Group Trials (RTOG) for glioblastoma multiforme and anaplastic astrocytoma. Int. J. Radiat. Oncol. Biol. Phys., *40:* 653–659, 1998.

16. Groves, M. D., Maor, M. H., Meyers, C., Kyritsis, A. P., Jaeckle, K. A., Yung, S. K. A., Sawaya, R. E., Hess, K., Bruner, J. M., Peterson, P., and Levin, V. A. A Phase II trial of high-dose bromodeoxyuridine with accelerated fractionation radiotherapy followed by Procarbazine,

Lomustine and Vincristine for glioblastoma multiforme. Int. J. Radiat. Oncol. Biol. Phys., *45:* 127–135, 1999.

17. Eisbruch, A., Robertson, J. M., Johnston, C. M., Tworek, J., Reynolds, K. R., Roberts, J. A., and Lawrence T. S. Bromodeoxyuridine alternating with radiation for advanced uterine cervix cancer: A Phase I and drug incorporation study. J. Clin. Oncol., *17:* 31–40, 1999.

18. Epstein, A. H., Lebovics, R. S., Goffman, T., Teague, D., Fuetsch, E. S., Glatstein, E., Okunieff, P., and Cook, J. A. Treatment of locally advanced cancer of the head and neck with 5′-iododeoxyuridine and hyperfractionated radiation therapy: measurement of cell labeling and thymidine replacement. J. Natl. Cancer Inst., *86:* 1775–1780, 1994.

19. Sondak, V. K., Robertson, J. M., Sussman, J. J., Saran, P. A., Chang, A. E., and Lawrence, T. S. Preoperative idoxuridine and radiation for large soft tissue sarcomas: clinical results with five-year follow-up. Ann. Surg. Oncol., *5:* 106–112, 1998.

20. Chang, A. I., Collins, J. M., Speth, P. A. J., Smith, R., Walton, L., Begley, M. G., Glatstein, E., and Kinsella, T. J. A Phase I study of intra-arterial iododeoxyuridine in patients with colorectal liver metastases. J. Clin. Oncol., *6:* 718–724, 1989.

21. Knol, J., Walker, S., Robertson, J., Yang, Z., Deremer, S., Stetson, P., Ensminger, W., and Lawrence, T. Incorporation of 5-bromo-2′-deoxyuridine into colorectal liver metastases and liver in patient receiving a 7-day hepatic arterial infusion. Cancer Res., *55:* 3687–3691, 1995.

22. Kinsella, T. J., Kunugi, K. A., Vielhuber, K., McCullough, W., Liu, S-H., and Cheng Y-C. *In vivo* comparison of oral 5-iodo-2′-deoxyuridine and 5-iodo-2-pyrimidinone-2′-deoxyribose toxicity, pharmacokinetics, and DNA incorporation in athymic mouse tissues and a human colon cancer xenograft (HCT-116). Cancer Res., *54:* 2695–2700, 1994.

23. Kinsella, T. J., Kunugi, K. A., Vielhuber, K. A., Fowler, J., Fitzsimmons, M., and Collins, J. M. Preclinical evaluation of 5-iodo-2-pyrimidinone-2′-deoxyribose (IPdR) as a prodrug for IUdR-mediated tumor radiosensitization in mouse and human tissues. Clin. Cancer Res., *4:* 99–109, 1998.

24. Kinsella, T. J., Vielhuber, K. A., Kunugi, K. A., Schupp, J., Davis, T. W., and Sands, H. Pre-clinical toxicity and efficacy study of a 14-day schedule of oral 5-iodo-2-pyrimidinone-2′-deoxyribose (IPdR) as a prodrug for IUdR-radiosensitization in U251 human glioblastoma xenografts. Clin. Cancer Res., *6:* 1468–1475, 2000.

25. Efange, S. M. N., Alessi, E. M., Shih, H. C., Cheng, Y-C., and Bartos, T. J. Synthesis and biological activities of 2-pyrimidone nucleosides 2,5-halo-2-pyrimidone-2′-deoxyribonucleosides. J. Med. Chem., *28:* 904–910, 1985.

26. Lewandowski, G. A., and Cheng, Y-C. Mechanism and mode of action of 5-iodo-2-pyrimidinone-2′deoxyribonucleoside, a potent anti-herpes simplex virus compound, in herpes simplex virus-infected cells. Mol. Pharmacol., *39:* 27–33, 1990.

27. Chang, C-N., Doong, S-L., and Cheng, Y-C. Conversion of 5-iodo-2-pyrimidinone-2′-deoxyribose to 5-iodo-deoxyuridine by aldehyde oxidase: implications in hepatotropic drug design. Biochem. Pharmacol., *43:* 2269–2273, 1992.

28. United States Food and Drug Administration. Good Laboratory Practice Regulations, Final Rule 21 CFR Part 58, U.S. Govt. Printing Office, Washington, DC.

29. Organization for Economic Cooperation and Development. The OECD Principles of Good Laboratory Practice, Environment Monograph No. 45, ODECD, Paris, France, 1992.

30. Institute of Laboratory Animal Resources. Guide for the Care and Use of Laboratory Animals. Washington, DC: National Academy Press, 1996.

31. McCully, C., Balis, F., Bacher, J., Phillips, J., and Poplack, D. A rhesus monkey model for continuous infusion of drugs into cerebrospinal fluid. Lab. Anim. Sci., *40:* 522–525, 1990.

32. Belanger, K., Collins, J. M., and Klecker, R. W., Jr. Technique for detection of DNA nucleobases by reverse-phase high performance liquid chromatography optimized for quantitative determination of thymidine substitution by iododeoxyuridine. J. Chromotogr., *417:* 57–63, 1987.

33. Kinsella, T. J., Collins, J., Rowland, J., Klecker, R., Wright, D., Katz, D., Steinberg, S. M., and Glatstein, E. Pharmacology and Phase I/II study of continuous intravenous infusions of iododeoxyuridine (IdUrd) and hyperfractionated radiotherapy in patients with glioblastoma multiforme. J. Clin. Oncol., *6:* 871–879, 1988.

34. Speth, P. A. J., Kinsella, T. J., Belanger, K., Klecker, R. W., Jr., Smith, R., Rowland, J., and Collins, J. M. Fluorodeoxyuridine modulation of the incorporation of iododeoxyuridine into DNA of granulocytes: A Phase I and clinical pharmacological study. Cancer Res., *48:* 2933–2937, 1988.

35. Yoshihara, S., and Taksumi, K. Purification and characterization of hepatic aldehyde oxidase in male and female mice. Arch. Biochem. Biophys., *338:* 29–34, 1997.

36. Wright, R. M., Clayton, D. A., Riley, M. G., McManaman, J. L., and Repine, J. E. cDNA cloning, sequencing, and characterization of male and female rat liver aldehyde oxidase (rAOX1). J. Biol. Chem., *274:* 3878–3886, 1999.

37. Kurosaki, M., Demontis, S., Barzago, M. M., Garattini, E., and Terao, M. Molecular cloning of the cDNA for mouse aldehyde oxidase: tissue distribution and regulation *in vivo* by testosterone. Biochem. J., *341:* 71–80, 1999.

38. Sugihara, K., Kitamura, S., Taksumi, K., Asahara, T., and Dohi, K. Differences in aldehyde oxidase activity in cytosolic preparations of human and monkey liver. Biochem. Mol. Biol. Int., *41:* 1153–1160, 1997.

Clinical Cancer Research

Preclinical Study of the Systemic Toxicity and Pharmacokinetics of 5-Iodo-2-deoxypyrimidinone-2′-deoxyribose as a Radiosensitizing Prodrug in Two, Non-Rodent Animal Species: Implications for Phase I Study Design

Timothy J. Kinsella, Jane E. Schupp, Thomas W. Davis, et al.

Clin Cancer Res 2000;6:3670-3679.